The Journal of Chemical Physics

Measurements of ultrafast dissociation in resonant inelastic x-ray scattering of water

Cite as: J. Chem. Phys. **150**, 204201 (2019); https://doi.org/10.1063/1.5081886
Submitted: 17 November 2018 . Accepted: 07 May 2019 . Published Online: 30 May 2019

Kosuke Yamazoe, Jun Miyawaki, Hideharu Niwa, Anders Nilsson, and Yoshihisa Harada

The Journal of Chemical Physics ARTICLE scitation.org/journal/jcp

Measurements of ultrafast dissociation in resonant inelastic x-ray scattering of water

Cite as: J. Chem. Phys. 150, 204201 (2019); doi: 10.1063/1.5081886
Submitted: 17 November 2018 • Accepted: 7 May 2019 •
Published Online: 30 May 2019

Kosuke Yamazoe,[1,2] Jun Miyawaki,[1,2,3] Hideharu Niwa,[1,3,a)] Anders Nilsson,[4,b)] and Yoshihisa Harada[1,2,3,b)]

AFFILIATIONS

[1]Institute for Solid State Physics (ISSP), The University of Tokyo, 5-1-5, Kashiwanoha, Kashiwa, Chiba 277-8581, Japan
[2]Department of Advanced Materials Science, Graduate School of Frontier Sciences, The University of Tokyo, 5-1-5, Kashiwanoha, Kashiwa, Chiba 277-8561, Japan
[3]Synchrotron Radiation Research Organization, The University of Tokyo, Tatsuno, Hyogo 679-5165, Japan
[4]Department of Physics, AlbaNova University Center, Stockholm University, SE-106 91 Stockholm, Sweden

[a)]**Present Address:** Division of Physics, Faculty of Pure and Applied Sciences, University of Tsukuba, 1-1-1 Tennodai, Tsukuba, Ibaraki 305-8577, Japan.
[b)]**Authors to whom correspondence should be addressed:** harada@issp.u-tokyo.ac.jp and andersn@fysik.su.se

ABSTRACT

There has been a discussion on the interpretation of the resonant inelastic x-ray scattering (RIXS) spectra of liquid water in terms of either different structural environments or that core hole dynamics can generate well-resolved dissociative spectral components. We have used RIXS with high resolution in the OH stretch vibration energy part, at extremely high overtones going toward the continuum of full OH bond breakage, to identify the amount of dissociative contributions in the valence band RIXS spectra at different excitation energies. We observe that at low excitation energies, corresponding to population of states with strongly antibonding character, the valence band RIXS spectra have a large contribution from a well-resolved dissociative feature. Instead, at higher excitations, this spectral component diminishes and becomes a weak structure on the high-energy side of one of the spectral peaks related to the $1b_1$ state from tetrahedral configurations. This result brings both interpretations to be essential for the understanding of RIXS spectra of liquid water.

INTRODUCTION

In order to explain over 70 unusual properties of water,[1] it has been proposed that there are fluctuations in water at ambient conditions between two local environments that have distinctly different structures. The dominating local motifs at ambient pressures have been proposed to consist mostly of close-packed, high-density liquid (HDL) local structures,[2–6] also denoted normal, thermally excited structures,[7] where some hydrogen bonds (H-bonds) are strongly modified to allow higher coordination. Upon cooling from high temperatures, patches of tetrahedrally coordinated molecules, often denoted low-density liquid (LDL),[2,8] symmetrical[9,10] or locally favored structures,[7] begin to appear as fluctuations in the HDL random structure. The number of such LDL patches and their size and lifetime would increase with decreasing temperature[2,3] and make the properties of water deviate from the simple liquid behavior at high temperatures.[2,7,11,12]

It is essential to provide experimental evidence of the existence of the two HDL-LDL environments in water and how these change as a function of temperature, pressure, and presence of solutes. The electronic structure probe of the occupied orbitals, x-ray emission spectroscopy (XES) or also often denoted resonant inelastic x-ray scattering (RIXS), shows for water that the highest occupied orbital $1b_1$ is split into two components $1b_1'$ and $1b_1''$;[13,14] see Fig. 1.

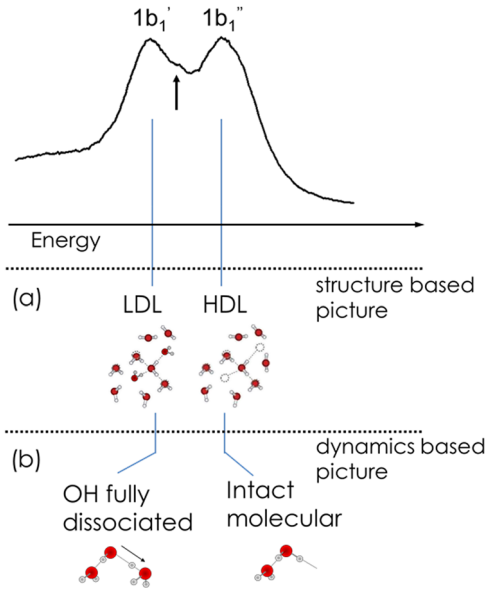

FIG. 1. The two dominant peaks in the $1b_1$ region have two different pictures; (a) two structural motifs referring to low density liquid (LDL) and high density liquid (HDL) environments; and (b) dissociative model where dynamics give rise to one peak as OH and the other intact H_2O. Black arrow indicates the faint spectral plateau at the higher part of the $1b_1'$ peak.

The origin of the split has been discussed as due to two different instantaneous structural environments giving different electronic emission energies in the spectroscopic process[14–16] where the low energy peak $1b_1'$ is related to LDL and the high energy peak $1b_1''$ as the HDL structural motifs.[3] However, the intensity variation of the two peaks in the $1b_1$ region between H_2O and D_2O is significantly larger than any structural dependence between the isotopes, indicating that there are important core hole induced vibrational effects affecting the spectra.[13,14] This core hole dynamics effect was included by applying an asymmetric Gaussian tail to higher loss energy of the $1b_1''$ peak by considering gradual energy shift of the emission line during the lifetime of the core hole. The $1b_1'$ peak would then reside on top of the asymmetry from the $1b_1''$ peak, and since the level of $1b_1''$ asymmetry would be isotope dependent, this would cause the two peaks to have different intensities.[15–17] We note that recent RIXS calculations of different structural environments in the liquid give rise to the shift between the two lone pair peaks.[18]

The alternative picture is that the core hole dynamics is considered more dominating and gives rise not only to asymmetrical line shape differences but also to a separate peak. Then, the two peaks in the $1b_1$ region are related to the extreme case with a fully dissociated OH lone pair state corresponding to the $1b_1'$ position due to faster dissociation of the hydrogen atom than the lifetime of the core hole and the $1b_1$ state of intact water at the $1b_1''$ position in Fig. 1.[13]

A validation of this interpretation was given based on molecular dynamics simulations of water followed with core hole dynamics calculations.[19–22] A peak appears in the simulated $1b_1'$ region that was assigned to dissociated fragments of a_1 symmetry. This interpretation was discussed in a review on RIXS applied to water[15] and found to be inconsistent based on two different experimental independent observations. First, polarization-dependent RIXS measurements show that this peak is not of a_1 but of b_1 symmetry.[23] Second, in the simulation, $1b_1''$ is kept at fixed energy position during the dynamics[20–22] and this would imply that there is no shift or change in line shape of the $1b_1''$ peak between the two isotopes. Indeed, there is a significant shift to lower emission energy and broader peak in H_2O in comparison with D_2O[14,17] showing that the lone pair peak should shift down in energy during the core hole dynamics. This is the basis for the asymmetry of the $1b_1''$ peak.[17] The simulations, proposing the a_1 symmetry peak, lead to that $3a_1$ intensity moves up in energy and appears in the lone pair region. Indeed, with a correct energy scale, the $3a_1$ emission peak should broaden and stay in the a_1 region separated by 2 eV from the $1b_1''$ peak.[17] Since this interpretation considering a_1 contribution to the lone pair region is not consistent with two previous experimental observations, we will no longer include it in the following discussion.

Here, we provide additional information on the debate of the two different interpretations shown in Fig. 1 using combined analysis of vibrational excitations in the elastic scattering region and valence band emissions in resonant inelastic x-ray scattering (RIXS) spectra. The high spectral resolution enables us to observe the vibrational losses going into the continuum of full OH bond breaking in the RIXS spectra upon selective excitation. This allows us to determine the amount of extremely enlarged O–H bond length states contributing to the $1b_1$ region of the RIXS spectra, which can be associated with a faint spectral plateau at the higher part of the $1b_1'$ peak. The latter is also shown to be consistent with the energy position of the OH^- ion in water. This means that the actual effect of core hole dynamics appears not only as the asymmetric tail to higher loss energy of the $1b_1''$ peak but also as a faint plateau that was not considered in the previous studies.[14–19] We assign three spectral features in the $1b_1$ region providing an important additional piece of information where the $1b_1'$ feature has two contributions, LDL structural environments and dissociative component coming from the dominated HDL environment where the latter is slightly shifted to higher energy. The $1b_1''$ peak is then associated with the mostly intact HDL.

METHODS

O 1*s* RIXS spectra of pure liquid H_2O water were collected with the high resolution soft X-ray emission spectrometer HORNET station at SPring-8 BL07LSU,[24] which is equipped with a high resolution soft x-ray RIXS spectrometer[25] perpendicular to the light path of the incident x-rays. The O 1*s* x-ray absorption spectrum (XAS) spectra were recorded with partial fluorescence yield mode using a 10 mm^2 Silicon Drift Detector (SDD, Ourstex, Co. Ltd.). The energy resolution for the O 1*s* XAS and XES measurements was 0.1 eV and 0.15 eV, respectively. A custom-made liquid flow-through cell equipped with a 150 nm thick SiC membrane (NTT-AT Corporation, Japan) was used to flush liquid water at a speed of 100 mm/s in the horizontal direction. The details of the experimental setup and operating condition are described elsewhere.[16] All measurements were done at room temperature.

RESULTS AND DISCUSSION

It has been demonstrated that it is possible to resolve vibrational spectra using high resolution RIXS at the O K-edge as an energy-loss process from the elastic line[26–29] and OH stretch vibrational spectra of water could be measured with RIXS.[28,30,31] Figure 2(a) shows the excitation-dependent vibrationally-resolved RIXS spectra of water related to the OH stretch. In the core-excited state, the potential energy surface is different from that of the ground state, and since the lifetime of the O 1*s* core-hole state is around 4 fs,[32] there is sufficient time for the vibrational wave packet to evolve along the internal O–H bond resulting in a large number of overtones. In water, it has been possible to detect excitations into v = 7 while beyond a continuum is seen, meaning that the decay is into the ground state above the dissociation limit where the OH bond is broken.[30]

Figure 2(a) shows how the amount of overtones depends strongly on the excitation energy. This is connected to the elongation of the OH bond in water during the 4 fs lifetime of the core hole. If the excited electron is not trapped in a bound state and is above the ionization limit, the excited electron could access the continuum of core-ionized states and delocalize into the liquid far from the core excited atom.[33] This process would then strongly affect the lifetime of the excited state at the core hole atom and will become much shorter than the core hole lifetime resulting in that the OH bond would not have time to elongate. We can thereby separate two contributions that will affect the amount of overtones in the spectra in terms of degree of OH elongation and lifetime of the excited electron compared to the existence of the core hole. The latter contribution will only become essential when the excitation energy is at or above the core ionization energy of water at around 538 eV.[34]

The x-ray absorption spectrum (XAS) of water is shown in Fig. 2(b) and has been categorized into three major spectral features in terms of the pre- (534–535 eV), main- (537–538 eV) and post-edge (540–541 eV) resonances.[35–37] In Fig. 2(b), we also show the integrated intensity of the plateau region of the vibrational loss between 4.0 eV and 4.5 eV taken from Fig. 2(a) as a function of excitation energy. This is similar to the study in liquid methanol,[38] but in this case, we are beyond any vibrational fine structure and thereby above the dissociation limit. By integrating 200 points included between 4.0 and 4.5 eV, the statistical error is fully minimized, which is indicated by the absence of the error bar masked by the marker of the tail intensity in Fig. 2(b).

We see at the pre-edge feature around 535 eV in the XAS process that we have a maximum of the intensity and thereby large number of dissociation events. This is expected since the pre-edge corresponds to excitation into strongly OH antibonding molecular orbitals of the water molecule causing large OH distortions, not only from the presence of the core hole but also due to the excited electron.[30,33,36,37] When we excite into resonances around the main-edge at 536–537 eV, the tail intensity rapidly decreases by a factor of 5 in comparison with the pre-edge. In this case, the excited electron is populating much less antibonding molecular character and the OH elongation is mostly driven by the core hole. From an inspection of Fig. 2(a), we observe that the intensities are more in the lower overtones in comparison with the pre-edge excitation.

As the excitation energy is further increased above 537.5 eV, the tail intensity completely diminishes as we are reaching the ionization limit. When the ionization channel opens, there is a possibility for a decay of the core excited state to the core ionized state, where the excited electron will be lost into the surrounding water. Such a process becomes possible when the core ionized state is at lower energy than the excited state. If the decay process into the core ionized state is faster than the core hole lifetime, this channel will dominate and no vibrational excitations will be seen close to the elastic line. Such a fast decay of the core excited state has been previously observed

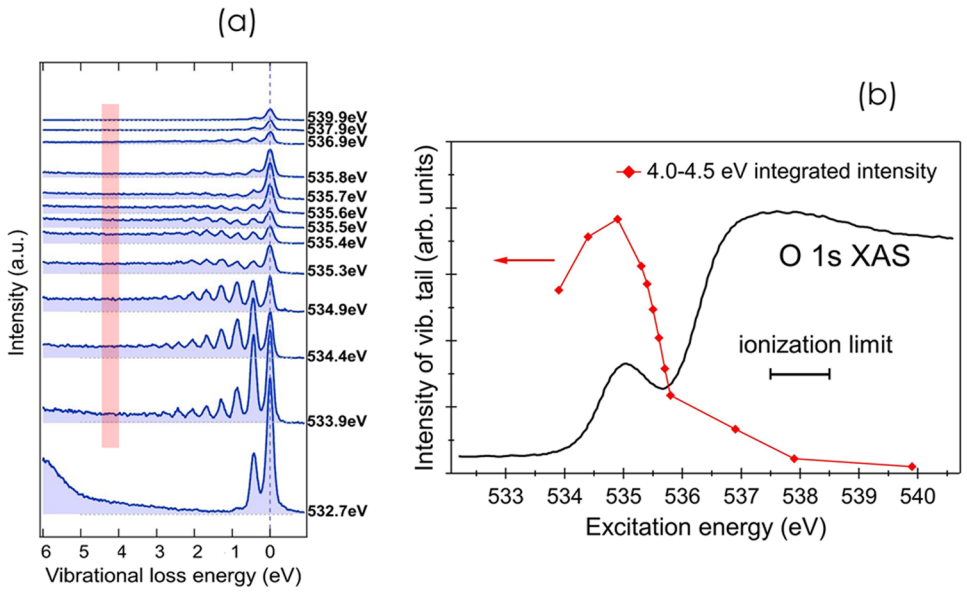

FIG. 2. (a) Excitation energy dependence of vibrationally resolved RIXS spectra reflecting multiple OH stretch excitations. (b) Integrated intensity of the vibrational loss in the plateau region between 4.0 eV and 4.5 eV [indicated by red-hatched area in (a)] as a function of the excitation energy. Also plotted is the O 1*s* XAS spectrum of liquid water.

in resonant Auger studies when the excitation energy is above the ionization limit through a loss of spectator shift from the excited electron.[33]

A consistency test of our overall interpretation can be seen in Fig. 2(a) by going far below the pre-edge at 532.7 eV where the scattering duration time becomes extremely short[39] and the overtones completely vanish similar to as for excitation energies above the core ionization limit where instead the decay into the core ionized state becomes faster. This is fully in line with what was observed for liquid methanol.[38]

In order to be as quantitative as possible, we have taken self-absorption effects for the plateau region into account but found them to be negligible in this case because at excitation energies under the ionization limit (538 eV excitation), the plateau energy is below 534 eV, which is prior to the absorption edge. Thus, we have now a direct measurement of the relative amount of dissociation events if we stay below the core ionized limit and this varies by a factor of 5 between excitation energies at the pre-edge and just below the ionization limit.

Since the tail intensity would point to the existence of a small component of a dissociated fragment or molecular species with a significantly elongated O–H bond, it is essential to discuss if this can be seen in the electronic transitions of the RIXS spectra. Here, we present new measurements that are similar to previous work[14,23,35] but with improved energy resolution and better control of the emission energy scale in order to see small shifts. We will introduce the hypothesis of an additional component in the excitation energy spectra and see if this is consistent with the tail intensity in Fig. 2(b).

Figure 3 shows the excitation-dependent RIXS spectra of the $1b_1$ region. The dissociative component is labeled $1b_1''^*$. If we start with the spectra at the onset of the pre-edge XAS resonance at 534.9 eV, there are two peaks. In the gas phase, RIXS spectra excited to the $4a_1$ state and also two peaks are observed where there is a large isotope effect in the relative intensity.[40] This has been proposed to be due to a dissociative peak at low energy and an intact water molecule,[40] which is fully consistent with a resonant Auger study of gas phase water excited to the same resonance where dissociative fragments have been detected[41] and theoretically simulated.[42] This is not surprising since the $4a_1$ molecular orbital is strongly antibonding along the OH bonds in the water molecule.[42] What is interesting is that for the pre-edge excited liquid water and $4a_1$ excited gas phase water, RIXS spectra closely resemble each other with the two peaks of similar intensity ratio and dependence between the isotopes.[15] These observations point to that the low-energy peak in the pre-edge excited RIXS spectrum of liquid water corresponds to a dissociative peak.[15] Another evidence for this can be derived from the lower part of the RIXS spectra between the $3a_1$ and $1b_2$ spectral feature where the $4a_1$ excited gas phase spectrum shows a sharp feature at 522 eV that is much stronger for H_2O than for D_2O corresponding to the σ bonding state of the remaining OH fragment after dissociation by core hole dynamics.[40] Such a spectral feature is also observed in the pre-edge excited water spectrum that has less intensity in D_2O showing also the existence of dissociation during the core hole lifetime.[15]

This observation of clear dissociation in pre-edge excited RIXS spectra is fully consistent with the discussion of Fig. 2 where strong tail intensity is seen in the vibrationally resolved spectra. Then, we use the pre-edge excited RIXS spectrum as a starting point to the

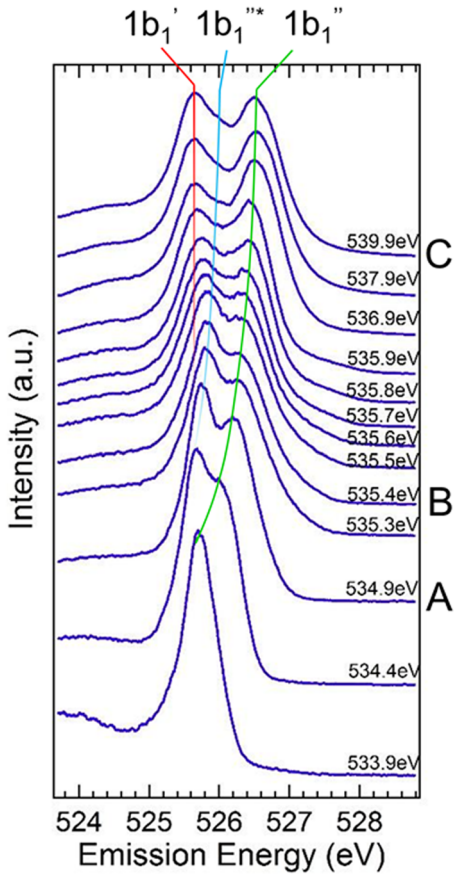

FIG. 3. Excitation energy dependence of O 1*s* valence emission spectra of liquid H_2O water in the $1b_1$ region. The red vertical bar indicates the $1b_1'$ component position that is independent of excitation energy; the green and light blue curves indicate $1b_1''$ components decomposed into two, one asymmetric Gaussian component with lower energy tail and the other a hump structure ($1b_1''^*$), respectively, which disperse to higher energy upon increase in the excitation energy.

apparent hypothesized dissociative (light blue) water component. Curve fitting of the pre-edge excited water spectrum is shown in panel A in Fig. 4(a) into two components, dissociative (light blue) and intact (green) water components.

We follow the energy position of these components as the excitation energy is changed, as shown in Fig. 3 where lines indicate their position. The $1b_1'$ peak (green, here assigned to intact HDL water) disperses strongly with photon energy between 533.9 eV and 535.3 eV and then much less up to 537.9 eV where it becomes constant at higher excitation energies. It is well known for many systems that for electrons excited into bound states, the spectra shift down in energy due to the difference in the screening of the core hole and valence hole by the additional electron.[29,43,44] Furthermore, varying the excitation energy involves variation of the population of the vibrational states in the excited pre-edge state that also can give different population of the vibrational states in the final $1b_1$ state of the intact molecule peak. For the dissociative component (light blue),

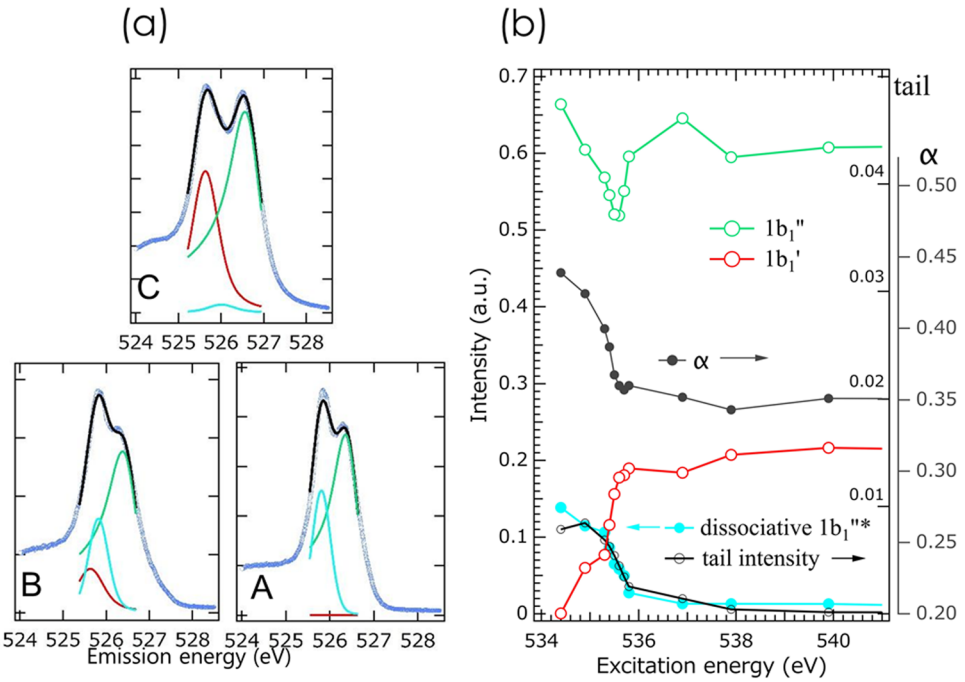

FIG. 4. Decomposition of the $1b_1$ profile using three components indicated in (a) for three selected excitation energies, A: 534.9 eV, B: 535.4 eV, and C: 539.9 eV. The fitting area is from 525.2 eV to 527.0 eV. (b) Intensity profile of the three components $1b_1'$ (red), $1b_1''$ with its asymmetry parameter α (green), and the dissociative component $1b_1''^*$ (light blue) compared with the integrated tail intensity of the vibrational progression (black) as plotted in Fig. 2(b).

we see even a smaller dispersion, and this can be understood as an additional degree of freedom to give a part of the excitation energy to the repelled hydrogen atom, and since we are only detecting the OH fragment in the RIXS process, there are smaller spectator shifts and vibrational excitations coupled to the valence emission for this fragment.[42]

In order to further assist in the spectra interpretation and test the consistency with the additional hypothesized dissociative component, together with the results from the tail intensity variation, we test if the spectra could be fitted using these 3 components. This is not a completely unique fit since more input would be required but is rather meant to test our hypothesis. Taking the reasonable variation of the three peak positions, we performed three component fittings to the XES spectra at all excitation energies, which are summarized in Fig. S1 along with the detailed procedure in the supplementary material, and results for three selected excitation energies are shown in Fig. 4(a). For the $1b_1''$ peak, we have introduced an asymmetry parameter[16] to describe the effect that core hole dynamics have on the line shape. It resembles closely the line shape of the almost exact solution to the Kramers-Heisenberg description of the water dimer.[17]

As the excitation energy increases above the pre-edge [Fig. 4(a) and Fig. S1], the dissociative component becomes much smaller in intensity, consistent with drop in tail intensity, seen in Fig. 2. It is interesting to note that this is almost opposite to what was found in the case of liquid methanol, where instead the tail intensity increased at higher excitation energy well above the pre-edge.[38]

In the lower part of Fig 4(b), we show the intensity of the fitted dissociative component (light blue) together with the tail intensity (black) from Fig. 2(b) as a function of excitation energy. We observe a close agreement indicating the consistency between the two. We can thereby conclude that a fitted third dissociative component that follows the tail intensity is consistent with the spectra. In particular, at excitation energies above the pre-edge, it decreases by almost a factor of 5 in contribution to the spectral profile. We note that the asymmetry parameter α also varies with excitation energy being higher at the pre-edge, fully consistent with the argument that this is related to core hole dynamics. Higher amount of the dissociative component gives higher asymmetry reflecting states with elongated O–H bond distances. It is this asymmetry that gives rise to the isotope effect at high excitation energies since it is much smaller for D_2O than for H_2O.[14–17] We see in Fig. 4(b) also how the $1b_1'$ spectral intensity (red) increases rapidly above the pre-edge, and this can be directly understood in terms of LDL related tetrahedral structures since it is expected that these lack pre-edge intensity as seen in XAS measurements of ice with minimum beam induced effects.[45]

It has been proposed that the lone pair state in the OH spectrum from sodium hydroxide (NaOH) solution would match the $1b_1'$ spectral peak in the non-resonant RIXS spectrum of water as a support of the picture that this feature is entirely due to a dissociation event.[13] The question is if the reference OH group should be the OH^- ion or the OH radical state. In the ionization process, when an O 1*s* electron is removed, we are left with a H_2O^+ molecule and with the equivalent core approximation; it means that the molecule is close to a H_2F^+ species. Since F is extremely electronegative, the dissociation event will keep electrons on the fluorine atom with H^+ leaving to the other hydrogen bonded molecule. We are then left with an OH group that has a completely filled valence shell as an OH^- plus an O 1*s* hole. O 1*s* ionization of the OH^- will thereby lead to a similar electronic state. The only deviation from the simplicity of this comparison can be if the solvation of the remaining OH^- group

is dramatically different between NaOH and water, but we assume the difference in the bond length between OH^- and solvating water for these two cases is only less than a tenth of an angstrom and, therefore, this bond length adjustment should occur on similar time scales as a 1.8 Å transfer of a proton to neighboring water molecule.

In order to enhance the OH contribution, selective excitation was used on a pre-pre-edge feature at 533.5 eV. However, since selective excitation was used, we may expect also, as in the case of pure water, that there will be a spectator shift and the absolute energy position of the OH spectral component in the RIXS spectrum will depend on the exact excitation energy. In the bottom of Fig. 5, we demonstrate that the OH feature shifts with excitation energy in the RIXS spectra of NaOH illustrating the spectator shift. In order to establish the RIXS position of the OH lone pair state, it is essential to use nonresonant excitation. In the top part of Fig. 5, we compare pure water and 2M NaOH solution at nonresonant conditions with the excitation energy of 539.6 eV. We observe that the $1b_1'$ position shifts to higher energy and broadens in the NaOH solution indicating the appearance of another component. The difference between the spectra of NaOH and pure water reveals the spectral component of the OH lone pair state, as shown in the middle of Fig. 5. We find the position to be shifted by 0.22 eV from the $1b_1'$ position of pure water. It resides almost exactly at the same position, as the fitted dissociative component in Fig. 4(b). This shows consistency with the picture that indeed there is a dissociative OH related component in liquid water at 526.0 eV indicated by an arrow in Fig. 5.

In a special interface layer of water in contact with a hydrophilic brush, there is indeed a spectrum of the $1b_1'$ component present with only a small tail toward the $1b_1''$ position indicating that this component can be seen without the high energy spectral peak.[46] The IR spectrum shows a vibrational OH stretch frequency of 3200 cm^{-1}[46] consistent with that the sample with a sole $1b_1'$ position consists of fully H-bonded coordinated water similar to LDL. It is very unlikely that an almost sole $1b_1'$ spectral peak would only be assigned to a fully dissociative OH component without spectral intensity for an intact water peak. Instead this is related to the spectral feature of a unique structural environment.

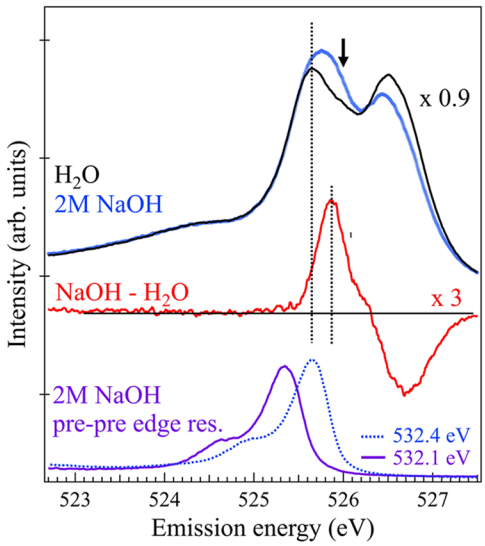

FIG. 5. Comparison of O 1*s* XES for 2M NaOH (blue) and pure H_2O (black) at 539.6 eV excitation energy, difference to extract the hydrated OH component (red), arrow indicates the fitted dissociative component from Fig. 4. At the bottom, two spectra (blue dotted and purple) indicate 2M NaOH spectra obtained around the pre-pre-edge resonance, by two different excitation energies 532.1 eV and 532.4 eV.

SUMMARY

In conclusion, we find that supporting evidence for both pictures, the one of two structural environments and the one of a dissociative component, contributes to the interpretation of high resolution RIXS data of liquid water. In particular, from the usage of the vibrationally resolved spectra, seen as losses from the elastic line, and inspecting the tail intensity, corresponding to the decay to an almost dissociated state, we can determine the spectral amount of such a component. At pre-edge excitation, the dissociative component is almost of equal intensity as the intact water component, but at higher excitation energies, it diminishes and is observed as a weak component on the high energy tail of the $1b_1'$ spectral peak. Based on these observations, we can confirm that the main part of the $1b_1'$ peak intensity is related to water in a tetrahedral structural environment.

SUPPLEMENTARY MATERIAL

See supplementary material for the details of the fitting procedure, comparison of the pre-edge excited gas-phase, liquid-phase RIXS spectra of H_2O water, and a zoomed image of the plateau region in Fig. 3.

ACKNOWLEDGMENTS

This work was carried out by joint research in the Synchrotron Radiation Research Organization and the Institute for Solid State Physics, The University of Tokyo (Proposal Nos. 2015B7403 and 2016A7507). We acknowledge financial support from the European Research Council (ERC advanced grant WATER under Project No. 667205) and the Swedish Research Council. We thank for valuable comments from Simon Schreck.

REFERENCES

[1] M. F. Chaplin, http://www1.lsbu.ac.uk/water/, 2015.
[2] A. Nilsson and L. G. M. Pettersson, "The structural origin of anomalous properties of liquid water," Nat. Commun. **6**, 8998 (2015).
[3] C. Huang *et al.*, "The inhomogeneous structure of water at ambient conditions," Proc. Natl. Acad. Sci. U. S. A. **106**, 15214–15218 (2009).
[4] O. Mishima and H. E. Stanley, "The relationship between liquid, supercooled and glassy water," Nature **396**, 329–335 (1998).
[5] A. K. Soper and M. A. Ricci, "Structures of high-density and low-density water," Phys. Rev. Lett. **84**, 2881–2884 (2000).
[6] M. C. Bellissent-Funel, "Is there a liquid-liquid phase transition in supercooled water?," Europhys. Lett. **42**, 161–166 (1998).
[7] J. Russo and H. Tanaka, "Understanding water's anomalies with locally favoured structures," Nat. Commun. **5**, 3556 (2014).
[8] A. Nilsson and L. G. M. Pettersson, "Perspective on the structure of liquid water," Chem. Phys. **389**, 1–34 (2011).

[9]T. D. Kühne and R. Z. Khaliullin, "Electronic signature of the instantaneous asymmetry in the first coordination shell of liquid water," Nat. Commun. **4**, 1450 (2013).
[10]M. Leetmaa *et al.*, "Diffraction and IR/Raman data do not prove tetrahedral water," J. Chem. Phys. **129**, 084502 (2008).
[11]P. Gallo *et al.*, "Water: A tale of two liquids," Chem. Rev. **116**, 7463–7500 (2016).
[12]V. Holten and M. A. Anisimov, "Entropy-driven liquid–liquid separation in supercooled water," Sci. Rep. **2**, 713 (2012).
[13]O. Fuchs *et al.*, "Isotope and temperature effects in liquid water probed by x-ray absorption and resonant x-ray emission spectroscopy," Phys. Rev. Lett. **100**, 027801 (2008).
[14]T. Tokushima *et al.*, "High resolution x-ray emission spectroscopy of liquid water: The observation of two structural motifs," Chem. Phys. Lett. **460**, 387–400 (2008).
[15]A. Nilsson *et al.*, "Resonant inelastic x-ray scattering of liquid water," J. Electron Spectrosc. Relat. Phenom. **188**, 84–100 (2013).
[16]T. Tokushima *et al.*, "High resolution x-ray emission spectroscopy of water and its assignment based on two structural motifs," J. Electron Spectrosc. Relat. Phenom. **177**, 192–205 (2010).
[17]M. P. Ljungberg, L. G. M. Pettersson, and A. Nilsson, "Vibrational interference effects in x-ray emission of a model water dimer: Implications for the interpretation of the liquid spectrum," J. Chem. Phys. **134**, 044513 (2011).
[18]I. Zhovtobriukh *et al.*, "Relationship between x-ray emission and absorption spectroscopy and the local H-bond environment in water," J. Chem. Phys. **148**, 144507 (2018).
[19]V. V. Cruz *et al.*, "Probing hydrogen bond strength in liquid water by resonant inelastic x-ray scattering," Nat. Commun. **10**, 1013 (2019).
[20]J. Niskanen *et al.*, "Compatibility of quantitative x-ray spectroscopy with continuous distribution models of water at ambient conditions," Proc. Natl. Acad. Sci. U. S. A. **116**, 4058–4063 (2019).
[21]M. Odelius, "Molecular dynamics simulations of fine structure in oxygen K-edge x-ray emission spectra of liquid water and ice," Phys. Rev. B **79**, 144204 (2009).
[22]M. Odelius, "Information content in O[1s] K-edge X-ray emission spectroscopy of liquid water," J. Phys. Chem. A **113**, 8176–8181 (2009).
[23]T. Tokushima *et al.*, "Polarization dependent resonant x-ray emission spectroscopy of D_2O and H_2O water: Assignment of the local molecular orbital symmetry," J. Chem. Phys. **136**, 044517 (2012).
[24]S. Yamamoto *et al.*, "New soft x-ray beamline BL07LSU at SPring-8," J. Synchrotron Radiat. **21**, 352–365 (2014).
[25]Y. Harada *et al.*, "Ultrahigh resolution soft x-ray emission spectrometer at BL07LSU in SPring-8," Rev. Sci. Instrum. **83**, 013116 (2012).
[26]R. C. Couto *et al.*, "Selective gating to vibrational modes through resonant x-ray scattering," Nat. Commun. **8**, 14165 (2017).
[27]F. Hennies *et al.*, "Resonant inelastic scattering spectra of free molecules with vibrational resolution," Phys. Rev. Lett. **104**, 193002 (2010).
[28]A. Pietzsch *et al.*, "Snapshots of the fluctuating hydrogen bond network in liquid water on the sub-femtosecond timescale with vibrational resonant inelastic x-ray scattering," Phys. Rev. Lett. **114**, 088302 (2015).
[29]J. E. Rubensson, "Resonant inelastic soft x-ray scattering applied to molecular materials," J. Electron Spectrosc. Relat. Phenom. **200**, 239–246 (2015).
[30]Y. Harada *et al.*, "Selective probing of the OH or OD stretch vibration in liquid water using resonant inelastic soft-x-ray scattering," Phys. Rev. Lett. **111**, 193001 (2013).
[31]Y. Harada *et al.*, "Probing the OH stretch in different local environments in liquid water," J. Phys. Chem. Lett. **8**, 5487–5491 (2017).
[32]M. Neeb *et al.*, "Coherent excitation of vibrational wave functions observed in core hole decay spectra of O_2, N_2 and CO," J. Electron Spectrosc. Relat. Phenom. **67**, 261–274 (1994).
[33]D. Nordlund *et al.*, "Probing the electron delocalization in liquid water and ice at attosecond time scales," Phys. Rev. Lett. **99**, 217406 (2007).
[34]B. Winter *et al.*, "Hydrogen bonds in liquid water studied by photoelectron spectroscopy," J. Chem. Phys. **126**, 124504 (2007).
[35]T. Fransson *et al.*, "X-ray and electron spectroscopy of water," Chem. Rev. **116**, 7551–7569 (2016).
[36]A. Nilsson *et al.*, "X-ray absorption spectroscopy and x-ray Raman scattering of water and ice; an experimental view," J. Electron Spectrosc. Relat. Phenom. **177**, 99–129 (2010).
[37]P. Wernet *et al.*, "The structure of the first coordination shell in liquid water," Science **304**, 995–999 (2004).
[38]S. Schreck *et al.*, "Dynamics of the OH group and the electronic structure of liquid alcohols," Struct. Dyn. **1**, 054901 (2014).
[39]R. Feifel *et al.*, "Generalization of the duration-time concept for interpreting high-resolution resonant photoemission spectra," Phys. Rev. A **69**, 022707 (2004).
[40]L. Weinhardt *et al.*, "Nuclear dynamics and spectator effects in resonant inelastic soft x-ray scattering of gas-phase water molecules," J. Chem. Phys. **136**, 144311 (2012).
[41]I. Hjelte *et al.*, "Evidence for ultra-fast dissociation of molecular water from resonant Auger spectroscopy," Chem. Phys. Lett. **334**, 151–158 (2001).
[42]O. Takahashi *et al.*, "Auger decay calculations with core-hole excited-state molecular-dynamics simulations of water," J. Chem. Phys. **124**, 064307 (2006).
[43]F. Gel'mukhanov and H. Ågren, "Resonant x-ray Raman scattering," Phys. Rep. **312**, 87–330 (1999).
[44]J.-E. Rubensson, "RIXS dynamics for beginners," J. Electron Spectrosc. Relat. Phenom. **110-111**, 135 (2000).
[45]J. A. Sellberg *et al.*, "Comparison of x-ray absorption spectra between water and ice: New ice data with low pre-edge absorption cross-section," J. Chem. Phys. **141**, 034507 (2014).
[46]K. Yamazoe *et al.*, "Enhancement of the hydrogen-bonding network of water confined in a polyelectrolyte brush," Langmuir **33**, 3954–3959 (2017).